Digital Object Identifier (DOI): 10.1109/PESGM.2015.7286090

Power & Energy Society General Meeting, 2015 IEEE; July 2015

Voltage and current balancing in Low and Medium Voltage grid by means of Smart Transformer

Giovanni De Carne
Giampaolo Buticchi
Marco Liserre
Changwoo Yoon
Frede Blaabjerg

Suggested Citation

G. De Carne, G. Buticchi, M. Liserre, C. Yoon and F. Blaabjerg, "Voltage and current balancing in Low and Medium Voltage grid by means of Smart Transformer," *2015 IEEE Power & Energy Society General Meeting*, Denver, CO, 2015, pp. 1-5.

Voltage and Current Balancing in Low and Medium Voltage Grid by means of Smart Transformer

Giovanni De Carne
Giampaolo Buticchi
Marco Liserre
Chair of Power Electronics
Kiel University
Kiel, Germany
gdc@tf.uni-kiel,de

Changwoo Yoon
Frede Blaabjerg
Department of Energy Technology
Aalborg University
Aalborg, Denmark
cyo@et.aau.dk

***Abstract*—The Smart Transformer (ST), which is a power electronics-based transformer, represents an enabling technology for providing new services to the Low Voltage (LV) and Medium Voltage (MV) grid. The 3-stage configuration, with a high frequency transformer and 2 DC links, allows the electrical separation of the LV and MV grids. This leads to the independence of the two grids: any disturbance downstream and upstream can be compensated and mitigated by the ST action, which is the case of the unbalanced load condition of the LV grids. The unbalanced currents demanded by the loads could create unbalanced voltages at the LV side and also unbalanced currents at the MV side of a traditional transformer. This paper presents the improvements achieved by ST implementation in terms of voltage and current balancing: with a proper control of the ST, it provides balanced voltage in the LV grid, demanding a balanced current from the MV grid. This feature increases the power quality in both grids and provides an improved service to the customers.**

***Index Terms*—Voltage Unbalance - Current Unbalance - Smart Transformer - Solid State Transformer**

I. Introduction

ST represents an enabling technology in the future distribution grids. The ST purpose is not just a simple substitution of the traditional transformer in the LV and MV voltage substations but it aims also to upgrade the distribution grid providing new services. The ST must prove to be efficient and reliable like the traditional transformer and at the same time flexible to adapt to fast grid changes. The ST allows more degrees of freedom for new control actions. Being a 3 stage converter based on power electronics, it allows electrical separation of the LV and MV grids [1]: they can act independently and they are connected physically by means of average active power exchange. This creates a "filtering effect" for the disturbances affecting the two grids: any disturbance (flicker, voltage sag, harmonics pollution) can be mitigated by the ST by means of a proper control and not transmitted to the other side. The traditional transformer does not have this enabling characteristic and also this represents a limiting factor for the grid improvement and hosting capabilities. At this regard, the unbalanced voltage conditions of the LV grids are source of problems to the Distribution System Operators (DSOs). An analytical way to measure the voltage unbalance with rms measurements is indicated in [2] and give as:

$$V_{unbalance}\% = 100 * \frac{max\left\{|V_{i,rms} - V_{avg}|\right\}}{V_{avg}} \quad \text{with} \quad i = a, b, c \tag{1}$$

where $V_{unbalance}\%$ is the voltage unbalance index in percent, $V_{i,rms}$ is the rms single-phase voltage, and V_{avg} is the average among the three single-phase voltages. This method is also recommended by [3] in the case of availability of voltage rms measurements and its values must be within the range of [0%-2%]. The unbalanced voltage conditions are coming from the presence of Distributed Generation (DG), new loads, like Battery Electric Vehicles (BEVs), or not balanced load distribution in the grid. The unbalanced voltage problem raised by the integration of small single-phase Photovoltaic (PV) power plants in the LV grid is e.g. presented in [4]. Depending on the installation distance of the PVs from the substation, the impact on the voltage unbalance can vary significantly. The scenario in [5] describes a case where the integration of BEVs has already reached high level in the LV grid. Investigating the voltage unbalance level during a long period, many violations of the limit imposed by the [3] have been found, mostly if the BEVs charging is not coordinated by any control algorithm. A detailed assessment on the impact of asymmetrical line geometry and unbalanced load on the voltage profiles is developed in [6]: it proposes a new load transposition method for mitigating the voltage unbalance. As explained in [7]–[9], the unbalanced voltage conditions impacts heavily on the motors (heating increase, torque pulsation, and reduction of lifespan). Wind turbines result be affected by unbalanced voltage conditions as well. In [10] has been explained how the Doubly Fed Induction Generators (DFIGs) are heavily affected from the voltage unbalances on the DC capacitors: the presence of the inverse sequence creates a 2nd harmonic oscillation on the DC link, impacting on the capacitor lifespan an reliability.

The traditional transformer cannot achieve improvement in case of unbalanced grids: the fixed winding ratio imposes unbalanced currents at the MV side if the LV side load distribution is unbalanced too. Consequently, the voltages

becomes unbalanced due to the non-uniform voltage drop in the grid. In this work the current unbalance is evaluated using the following formulation:

$$I_{unbalance}\% = 100 * \frac{|I_-|}{|I_+|} \quad (2)$$

where $I_{unbalance}\%$ is the current unbalance index in percent, $|I_-|$ is the inverse sequence current magnitude, and $|I_+|$ is the direct sequence current magnitude. In normal operating conditions, this ratio must be within the range [0%-30%], as suggested by [3].

This paper describes the improvements achieved with the ST implementation in the LV/MV grid substations in terms of balancing of voltage and current. Indeed the ST can provide balanced voltage when the grid is unbalanced and demands balanced current at the MV side. Section II depicts the control method adopted in this work; Section III describes briefly the Cigré 12-bus feeder grid [11] used for simulations and provides simulations using a traditional transformer; Section IV shows the simulation results when the ST has been implemented in the grid to demonstrate the improved performance. Finally, Section V is dedicated to the conclusions.

II. ST Concept and Control

The major feature of the ST is a power electronics interface with the grids [1]. The ST concept lies on the creation of a new control point between the LV and MV grids, enabling new possibilities in terms of grid optimization. The ST is composed of two grid connected inverters at the LV and MV sides and a Dual Active Bridge (DAB) converter, which is able to transform the voltage by means of an High Frequency (HF) transformer. The presence of the two DC link at the two different DAB converter sides enables the electrical separation of the grids, as anticipated in the previous section. Fig. 1 shows the ST concept by means of a single-line diagram:

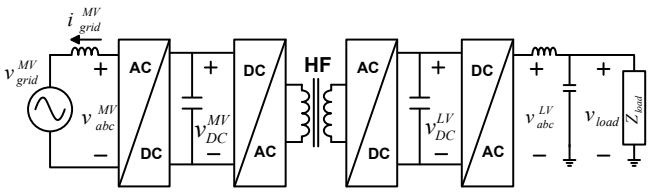

Fig. 1. ST 3-stage topology

In this paper an abc control method has been proposed for synthesizing the balanced voltage at the LV side, and demanding a balanced current at the MV side. The control is described in Fig. 2. The LV side controller is composed by a double loop: the inner one that imposes the voltage waveform following a voltage reference, created by an external one. Here a Proportional-Integral (PI) controller compensates the error between the rms voltage on the LV grid side and the reference value (i.e., here it is 230V rms). The output from the PI controller is multiplied by a sinusoidal waveform pulsating at 50 Hz, compared with the grid voltage and sent

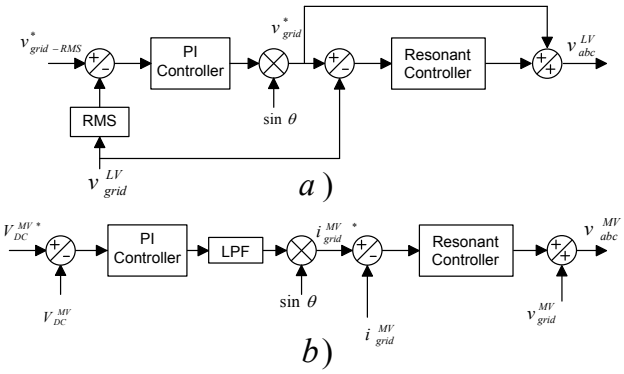

Fig. 2. ST a) voltage and b) current controller

to a Proportional-Resonant (PR) controller tuned at 50 Hz. The output is the corrective action to be added to the feed-forwarded grid voltage in order to have the voltage waveform that respects the voltage balancing requirements. The MV side controller works as a voltage-current loop: the ST measures the DC voltage at the MV capacitor and compares it with the rated voltage value. Here, a PI controller minimizes the error and sends the reference value to the AC side controller, filtered by a Low Pass Filter (LPF) in order to mitigate the quick set point variations. The new reference value obtained represents the reference current that must be applied at the MV side in order to keep constant the voltage in the MV DC link. This value is compared with the grid current and the error is sent to the resonant controller. As at the LV side, a voltage feed-forward signal is added to the compensated error. The voltage value calculated is the needed one in order to give the correct current amount from the MV grid.

III. Benchmark Grid

The benchmark grid used for showing the improvements achieved with the ST in the LV and MV grids is the LV Cigré 12-bus feeder [11] as shown in the single-line diagram in Fig. 3.

The grid has been simulated in PSCAD/EMTC and the simulation time window has been chosen of 100 seconds. This grid is composed by unbalanced passive loads, modeled as constant impedance; two photovoltaic power plants placed in nodes C and D; a fixed speed wind turbine, placed in node E; and two Battery Energy Storage Systems (BESSs) placed in nodes A and B. This grid represents a good benchmark for testing the unbalanced conditions of LV grid: the load is heavily unbalanced as it can be noticed by the current rms profiles in Fig. 4. The current unbalance leads to an unbalanced voltage drop, as shown in Fig. 5. The unbalanced conditions from the LV grid are transferred to the MV grid. Fig. 6 shows the unbalanced conditions in a time framework of 100 ms.

The unbalance trends are more evident if evaluated taking into account equations (1) for the LV grid voltages and (2) for the MV grid currents. Fig. 7 shows the characteristic of the aforementioned voltage index: although the values are still in the suggested range, they are high considering the small load

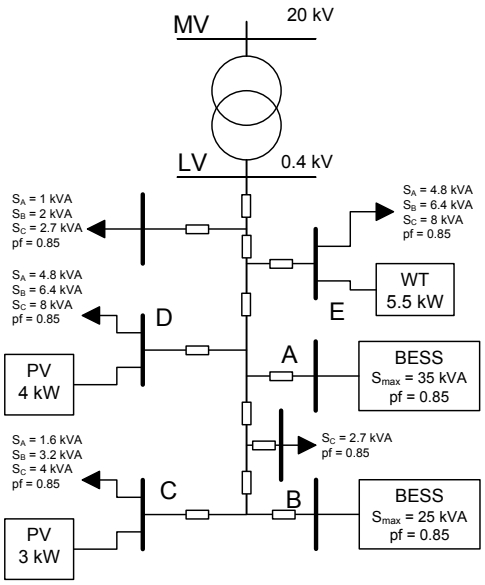

Fig. 3. LV Cigré 12-bus feeder [11]

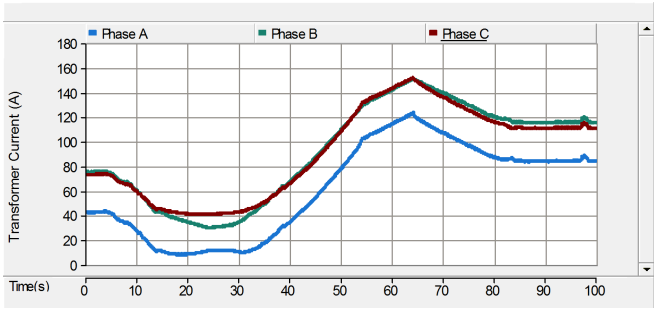

Fig. 4. LV line currents simulated in the Cigré model with traditional transformer: Phase A (blue line), Phase B (green line), Phase C (red line)

demanded in the studied grid. If the load tends to increase proportionally, the limit of 2% can easily be exceeded. Fig. 8 describes the MV current ratio values which are referred in eq.(2): the limit of 30% is exceeded for one third of the time, deteriorating the power quality in the MV grid.

In respect to the grid described above, to study the performance of the ST, several hypothesis have been done for the DG and the BESSs: 1) the photovoltaics are working with a power factor equal to unity and without any droop control; 2) a V-Q droop control has been implemented in the BESSs; 3) the active power profiles of the BESSs have been set independently from the grid state and they do not change varying the grid parameters. The DG and BESSs power profiles are shown in Fig. 9 and Fig. 10 respectively. Fig. 9 depicts the instantaneous active power of the photovoltaic plants and wind turbine. The DG power plants are small in size, so the contribution in terms of active power results be marginal. A greater power contribution is given by the BESSs, where Fig. 10 shows their active and reactive instantaneous power profiles.

The batteries are performing a charging-discharging power

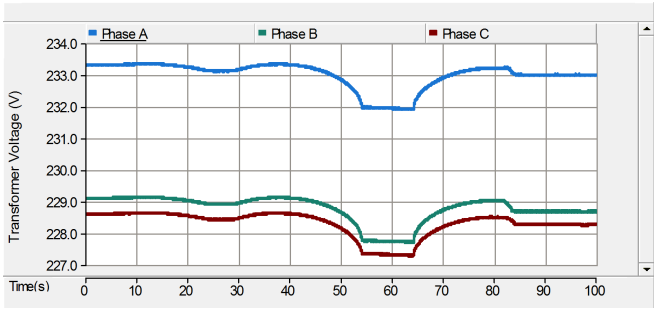

Fig. 5. LV line-to-ground voltages using a traditional transformer: Phase A (blue line), Phase B (green line), Phase C (red line)

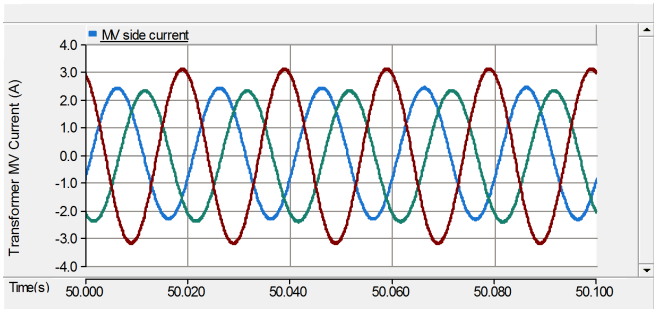

Fig. 6. MV line currents using a traditional transformer: Phase A (blue line), Phase B (green line), Phase C (red line)

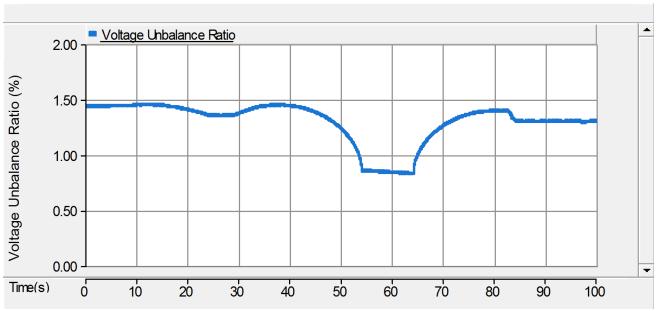

Fig. 7. Voltage Unbalance Ratio as given in eq.(1) using a traditional transformer

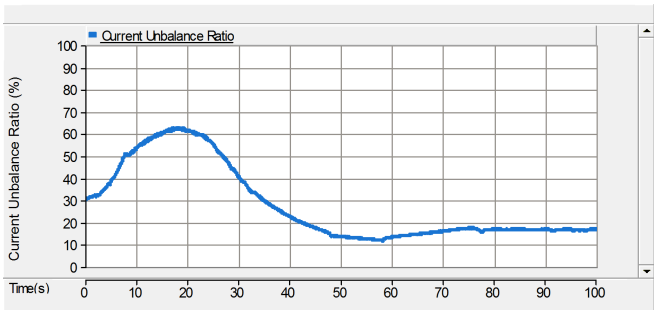

Fig. 8. Current Unbalance Ratio as given in eq.(2) using a traditional transformer

profile during the time window. The reactive power injected by the V-Q droop controllers, in order to improve the voltage

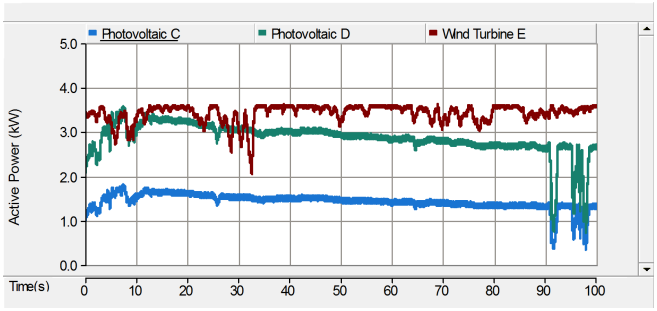

Fig. 9. DG active power using a traditional transformer: Photovoltaic in node C (blue line), Photovoltaic in node D (green line), Wind Turbine in node E (red line)

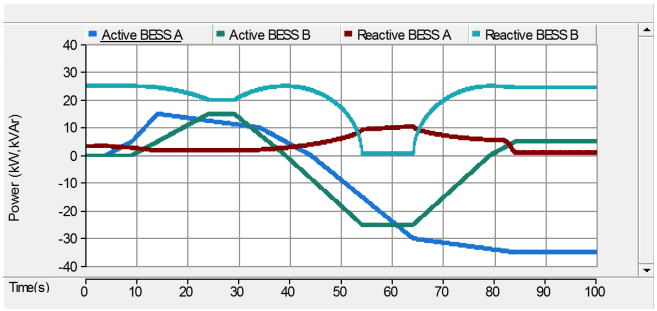

Fig. 10. Active and reactive power of BESSs in nodes A and B using a traditional transformer

value, depends on the active power set points: it must be in agreement with the batteries apparent power size. As it can be noticed in Fig. 10, the reactive power is not always available: working at maximum power as a load (within the range [55 s-65 s]), the BESS B limits the reactive power injection to zero. It results in a further reduction of the voltage magnitude in all of the phases. The active and reactive instantaneous power measured at the transformer level are represented in Fig. 11. The reactive power injected by the transformer is small, due to the V-Q droop controller operation in the grid.

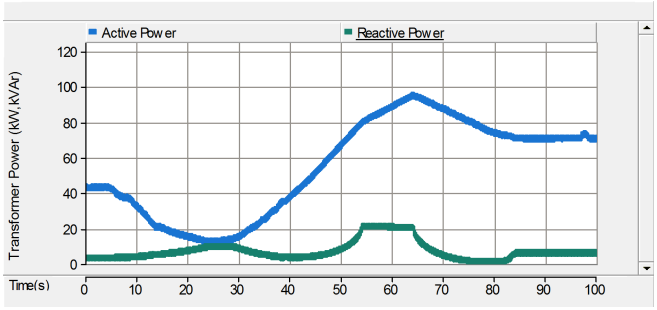

Fig. 11. Active and reactive power provided to the LV grid using a traditional transformer

IV. Simulation Results of ST

This Section describes the simulation results obtained by the ST implementation in the LV/MV substation and applying the control as described in Section II. With respect to the case of the traditional transformer, it compared the same load demand for a fair comparison and the same active power production by the DG and BESSs. The reactive power injection of BESSs changes accordingly with the V-Q droop controller operation, as depicted in Fig. 12. In this case, less reactive power has been injected with respect to the traditional transformer case. This is due to the improved ST voltage control, that fixes the voltage at substation level to 230 V. Fig. 12 shows how the BESS placed in node A injects only a limited amount of reactive power in the time window considered. Instead, the BESS taking place in node B, results be limited in the reactive power injection when the BESS maximum capability is reached. The lower request of reactive power at BESS level must be compensated by the ST. Indeed Fig. 13 shows how the reactive power injected in the grid at substation level is increased on average. Instead, the active power supplied by ST is practically unchanged.

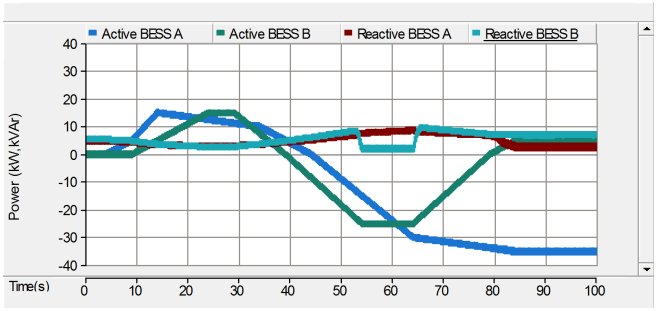

Fig. 12. Active and reactive power of BESSs in nodes A and B using a ST

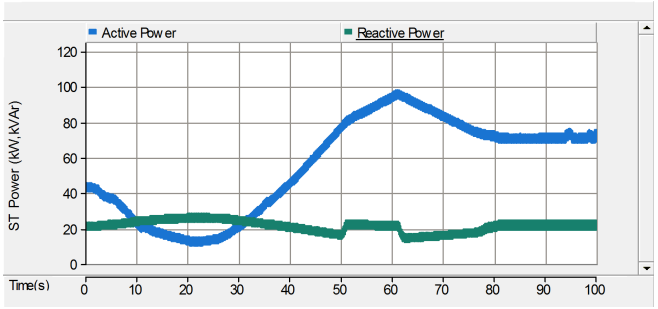

Fig. 13. Active and reactive power provided to the LV grid using a ST

Under the aforementioned considerations, the controller performs the control action for balancing the ST voltages: it can be noticed in Fig. 14 how the voltage is perfectly balanced for the whole simulation time, independently of the active and reactive power load request. Indeed, the demand of current at ST level is still unbalanced, as demonstrated in Fig. 15, but the voltage controller forces the ST to synthesize balanced voltages and thus the voltage unbalance index results to be near zero. It is worth to highlight the current profiles changing with respect to the traditional transformer case due to the different reactive power injection profile of the ST.

Applying the control proposed in Section II, the ST achieves balancing improvements also at the MV side. The proposed

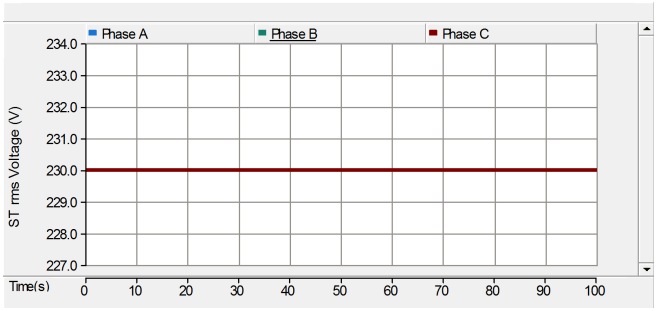

Fig. 14. LV line-to-ground voltages using a ST: Phase A (blue line), Phase B (green line), Phase C (red line)

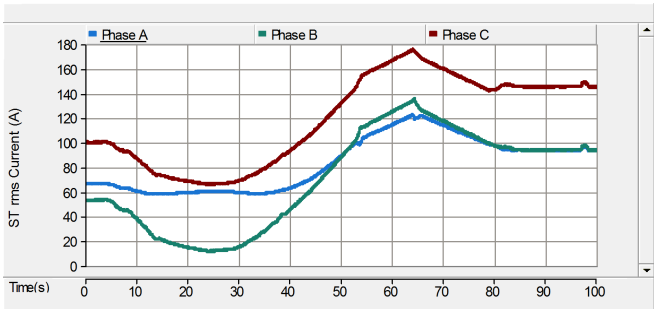

Fig. 15. LV line currents using a ST: Phase A (blue line), Phase B (green line), Phase C (red line)

controller shown in Fig. 2 enables the compensation of the unbalanced currents requested by the loads. The current profiles, as depicted in Fig. 16, are now perfectly balanced.

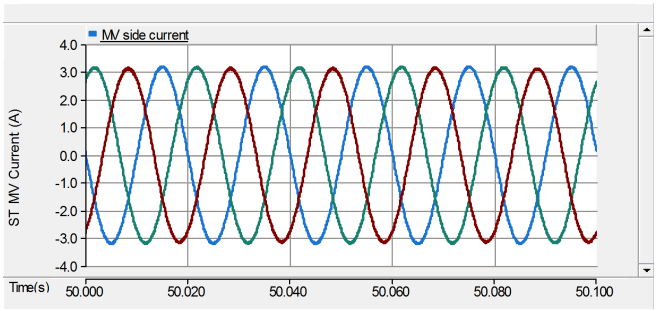

Fig. 16. MV line currents using a ST: Phase A (blue line), Phase B (green line), Phase C (red line)

This effect is better demonstrated considering the current unbalance index in Fig. 17: by using the ST the current unbalance ratio in MV grid is always below 4% for the whole considered period, instead of the peak over 60% achieved in the traditional transformer case as shown in Fig. 8.

V. Conclusion

This paper has studied one of the main services that the ST can provide to the distribution grid which is current and voltage balancing. The ST implemented in the LV/MV substations has filtering capabilities in respect to these grid disturbances. If an unbalanced condition is present in the LV grid, the ST can still provide perfectly balanced voltage profiles and demand balanced currents to the MV grid. Compared to the traditional transformer, the ST has demonstrated to increase significantly the power quality, both in LV and MV grids which increases the service quality to the customers.

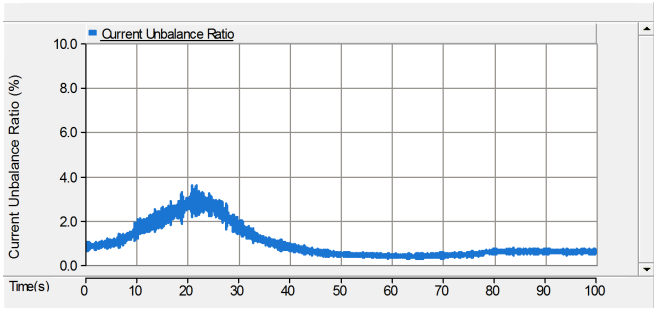

Fig. 17. Current Unbalance Ratio as given in eq.(2) using a ST

Acknowledgment

The research leading to these results has received funding from the European Research Council under the European Unions Seventh Framework Programme (FP/2007-2013) / ERC Grant Agreement n. [616344].

References

[1] R. Pena-Alzola, G. Gohil, L. Mathe, M. Liserre, and F. Blaabjerg, "Review of modular power converters solutions for smart transformer in distribution system," in *IEEE Energy Conversion Congress and Exposition (ECCE)*, Sept 2013, pp. 380–387.

[2] *ANSI C84.1-2006 American National Standard For Electric Power System and Equipment*, National Electrical Manufacturers Association Std.

[3] "Recommended pratice for monitoring electric power quality," *IEEE Std 1159-2009 (Revision of IEEE Std 1159-1995)*, pp. c1–81, June 2009.

[4] F. Shahnia, R. Majumder, A. Ghosh, G. Ledwich, and F. Zare, "Voltage imbalance analysis in residential low voltage distribution networks with rooftop {PVs}," *Electric Power Systems Research*, vol. 81, no. 9, pp. 1805 – 1814, 2011.

[5] N. Leemput, F. Geth, J. Van Roy, A. Delnooz, J. Buscher, and J. Driesen, "Impact of electric vehicle on-board single-phase charging strategies on a flemish residential grid," *IEEE Trans. on Smart Grid*, vol. 5, no. 4, pp. 1815–1822, July 2014.

[6] R. Yan and T. Saha, "Investigation of voltage imbalance due to distribution network unbalanced line configurations and load levels," *IEEE Trans. on Power Systems*, vol. 28, no. 2, pp. 1829–1838, May 2013.

[7] S. Duarte and N. Kagan, "A power-quality index to assess the impact of voltage harmonic distortions and unbalance to three-phase induction motors," *IEEE Trans. on Power Delivery*, vol. 25, no. 3, pp. 1846–1854, July 2010.

[8] J. Faiz, H. Ebrahimpour, and P. Pillay, "Influence of unbalanced voltage on the steady-state performance of a three-phase squirrel-cage induction motor," *IEEE Trans. on Energy Conversion*, vol. 19, no. 4, pp. 657–662, Dec 2004.

[9] P. Pillay and M. Manyage, "Loss of life in induction machines operating with unbalanced supplies," *IEEE Trans. on Energy Conversion*, vol. 21, no. 4, pp. 813–822, Dec 2006.

[10] C. Liu, D. Xu, N. Zhu, F. Blaabjerg, and M. Chen, "Dc-voltage fluctuation elimination through a dc-capacitor current control for dfig converters under unbalanced grid voltage conditions," *IEEE Trans. on Power Electronics*, vol. 28, no. 7, pp. 3206–3218, July 2013.

[11] "Benchmark system for network integration of renewable and distributed energy resources c06.04.02," CIGRE, Tech. Rep., 2014.